Cardiovascular Pathology 59 (2022) 107426

Contents lists available at ScienceDirect

Cardiovascular Pathology

journal homepage: www.elsevier.com/locate/carpath

Autonomic nerves in myocardial sleeves around caval veins: Potential role in cardiovascular mortality?

Denis Depes[a,b], Ari Mennander[b,c], Timo Paavonen[a,b], Ivana Kholová[a,b,*]

[a] Department of Pathology, Fimlab Laboratories, Arvo Ylpön katu 4, 33520 Tampere, Finland
[b] Faculty of Medicine and Health Technology, Tampere University, Arvo Ylpön katu 34, 33520 Tampere, Finland
[c] Division of Cardiothoracic Surgery, Tampere University Heart Hospital, Elämänaukio 1, 33520 Tampere, Finland

ARTICLE INFO

Article history:
Received 30 November 2021
Revised 24 March 2022
Accepted 26 March 2022

Keywords:
Caval vein
Myocardial sleeve
Nerve density
Autonomic nervous system
Atrial fibrillation
Cardiovascular death

ABSTRACT

Background: Quantitative changes in the cardiac autonomic nervous system may play an important role in the pathogenesis of various cardiovascular diseases. In the present morphological analysis, we aimed to study autonomic nerve density in myocardial sleeves and surrounding fibro-fatty tissue around caval veins. We correlated the nerve distribution with cardiovascular mortality and a history of atrial fibrillation.

Materials and Methods: A total of 24 autopsied adult hearts were excised together with the superior and inferior vena cava and grouped according to the immediate and underlying causes of death (cardiovascular vs. non-cardiovascular), and documented heart rhythm history (atrial fibrillation vs. sinus rhythm). The density of autonomic nerves was quantified by measuring the area of immunohistochemical staining for sympathetic (tyrosine hydroxylase, TH) and parasympathetic (choline acetyltransferase, CHAT) nerves and ganglia. Growth-associated protein 43 (GAP43) was used as a neural growth marker.

Results: The mean density of TH-positive nerves in the superior vena cava myocardial sleeves was significantly decreased between groups with documented underlying cardiovascular vs. non-cardiovascular cause of death (mean density ± standard deviation (SD): 704.81±1016.41 $\mu m^2/mm^2$ vs. 2391.01±1841.37 $\mu m^2/mm^2$; $P = .008$). Similarly, the nerve density of GAP43-positive nerves in the superior vena cava myocardial sleeves was significantly lower in subjects with documented underlying cardiovascular cause of death (mean density ± SD: 884.74±1240.16 $\mu m^2/mm^2$ vs. 2132.89±1845.89 $\mu m^2/mm^2$; $P = .040$). The mean age was significantly higher in subjects with documented underlying cardiovascular vs. non-cardiovascular cause of death (mean age ± SD: 69.2±11.9 years, vs. 57.5±11.2 years, $P = .016$). No differences were found in nerve densities of TH-positive (953.01±1042.93 $\mu m^2/mm^2$ vs. 919.26±1677.58 $\mu m^2/mm^2$), CHAT-positive (180.8±532.9 $\mu m^2/mm^2$ vs. 374.22±894.76 $\mu m^2/mm^2$), and GAP43-positive nerves (593.58±507.97 $\mu m^2/mm^2$ vs. 1337.34±1747.69 $\mu m^2/mm^2$) in myocardial sleeves around the inferior vena cava between groups with documented immediate cardiovascular vs. non-cardiovascular cause of death. Similarly, no differences were found between groups with documented underlying cardiovascular vs. non-cardiovascular cause of death (TH: 717.23±887.31 $\mu m^2/mm^2$ vs. 1365.51±2149.10 $\mu m^2/mm^2$; CHAT: 256.18±666.86 $\mu m^2/mm^2$ vs. 368.53±959.47 $\mu m^2/mm^2$; GAP43: 661.21±839.51 $\mu m^2/mm^2$ vs. 1759.90±2008.80 $\mu m^2/mm^2$). Moreover, there was no association found in nerve densities between subjects with documented atrial fibrillation vs. sinus rhythm (TH: 235.07±425.69 $\mu m^2/mm^2$ vs. 1166.08±1563.84 $\mu m^2/mm^2$; CHAT: 648.59±1017.33 $\mu m^2/mm^2$ vs. 175.31±641.65 $\mu m^2/mm^2$; GAP43: 990.17±1315.18 $\mu m^2/mm^2$ vs. 1039.86±1467.23 $\mu m^2/mm^2$).

Conclusions: Decrease of superior vena cava myocardial sleeve sympathetic nerves may be associated with cardiovascular mortality and/or aging. No difference in autonomic innervation was found between subjects with documented atrial fibrillation vs. sinus rhythm.

Abbreviations: SVC, superior vena cava; IVC, inferior vena cava; ANS, autonomic nervous system; CV, caval vein; TH, tyrosine hydroxylase; CHAT, choline acetyltransferase; GAP43, growth-associated protein 43; WS, whole section; MS, myocardial sleeves; FFT, fibro-fatty tissue.

* Corresponding author: Phone: +358331174851.
E-mail address: ivana.kholova@tuni.fi (I. Kholová).

https://doi.org/10.1016/j.carpath.2022.107426

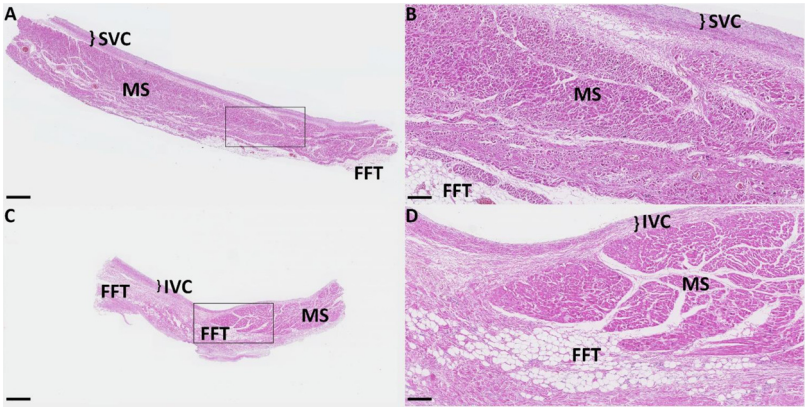

Fig. 1. Representative histological sections of myocardial sleeves around superior (SVC) and inferior vena cava (IVC). (A) Low-power histological section showing myocardial sleeve (MS) extending from the right atrium along SVC. A small amount of fibro-fatty tissue (FFT) surrounds the myocardium. HE stain, bar=1 mm. (B) Histological section showing magnified rectangular region from A. Dispersed mild fibrotic changes of the myocardial sleeve can be noted in the whole region. The myocardial fibers are arranged either circularly or longitudinally. HE stain, bar=200 µm. (C) Low-power histological section of IVC and MS along the outer aspect of the venous wall. Abundant FFT is seen around MS. HE stain, bar=1 mm. (D) Histological section showing magnified rectangular region from C. The tapering myocardium shows the distal portion of the MS around IVC. The myocardial fibers are arranged mostly circularly and are intermingled with rich FFT. HE stain, bar=200 µm.

1. Introduction

Myocardial sleeves are muscular extensions of cardiac atria covering the proximal outer parts of large cardiac veins [1]. The sleeves are thickest at the proximal end of the veins gradually tapering distally (Fig. 1) and are mainly known as sites of ectopic arrhythmogenic foci [2,3]. As shown in previous studies, myocardial sleeves are present in 76-78% of caval veins [1,4]. Previous research has established the importance of electrophysiologic [5,6] and morphologic [1,4] changes in the superior (SVC) and inferior vena cava (IVC) myocardial sleeves in the pathophysiology of cardiovascular diseases during arrhythmias. Myocardial sleeves around pulmonary veins have been studied earlier [7,8]. Although some research has been carried out on the canine hearts [9], no studies have investigated the autonomic nerve density of the SVC and IVC myocardial sleeves in human hearts.

The heart is innervated by the autonomic nervous system (ANS), which consists of the sympathetic and parasympathetic branches. Both branches innervate the whole heart and regulate balanced cardiac function via neurotransmitters and ion channel interactions. While sympathetic fibers increase heart rate, contractility, and atrioventricular conduction, parasympathetic fibers affect the heart conversely by slowing the heart rate and contractility [10].

Dysregulation of ANS has been studied in relation to the pathogenesis of various cardiovascular diseases including heart failure [11], myocardial ischemia [12], cardiac arrhythmias [13], and sudden cardiac death [14]. Previous studies have shown that chronic heart failure resulted in a decrease in sympathetic innervation and neural growth in the myocardium [15–17]. The density of TH- and GAP43-positive nerves in the atria increased in chronic myocardial ischemia cases [18]. Data from both human and animal studies suggest increased atrial ANS innervation and nerve sprouting as an arrhythmogenic substrate of atrial fibrillation (AF) [19–23]. These conditions may contribute to increased cardiovascular mortality.

The ANS nerve density quantitative changes as an autonomic remodeling function and its correlation to cardiovascular mortality have not been previously profoundly studied. This study aimed to investigate quantitative changes in ANS density of the SVC and IVC myocardial sleeves and surrounding fibro-fatty tissue by immunohistochemical and morphometrical analysis, and to correlate ANS density with immediate and underlying cause of death and a history of atrial fibrillation.

2. Materials and methods

2.1. Study population and sample collection

SVC and IVC samples were prospectively collected from 24 consecutive hospital adult autopsied hearts at the Fingerland Department of Pathology, Charles University Hospital, Hradec Králové, Czech Republic. The mean age of subjects ± standard deviation (SD) was 65.3±12.7 years; M:F ratio was 13:11; and mean heart weight ± SD was 450.4±110.4 grams. Hearts were excised together with SVC and IVC. SVC was then separated from the right atrium at the level of the sulcus terminalis at the base of the appendage, and IVC was separated at the angle with the bottom of the right atrium. Both atriovenous junctions were macroscopically determined. All CVs were cut longitudinally, spread, fixed in 10% buffered formalin, and processed into paraffin blocks. In total, 197 blocks of CV tissue were included in the study, ranging from 4 to 11 paraffin blocks per autopsy heart according to the heart size and CV length. The sinoatrial node was not collected in any case. The basic morphology of samples and the collection technique were described in detail previously [1].

Collection and further use of the material were approved by the Ethical Committee of the University Hospital, Hradec Králové, Czech Republic. The present study on the material was performed at Tampere University, Finland, with institutional approval from the Pirkanmaa Health Care District Ethical Committee (R15013). The study was performed in accordance with the Declaration of Helsinki.

2.2. Characterization of study groups

All 24 subjects were included in all three groups according to the documented immediate (group 1; n=24) and underlying (group 2; n=24) cause of death and history of atrial fibrillation (group 3; n=24). The groups were subdivided into subgroups, which were compared accordingly (A vs. B). The most prevalent immediate cause of death was cardiovascular (group 1A) (n=10), followed by various 14 non-cardiovascular causes (group 1B). Sixteen subjects were included in the underlying cardiovascular cause of death group (group 2A) and eight subjects were included in the documented underlying non-cardiovascular cause of death group (group 2B). According to the medical history of studied subjects, 6 subjects were diagnosed with atrial fibrillation (group 3A) and 18

Table 1a
Characteristics of studied subjects

ID no.	Age (years)	Sex	Heart weight (g)	Immediate cause of death (A: CVS, B: non-CVS) (group 1)		Underlying cause of death (A: CVS, B: non-CVS) (group 2)		Heart rhythm (A: AF, B: SR) (group 3)	
1	78	female	550	myocardial infarction	A	ASVD	A	SR	B
2	67	male	290	generalized carcinoma	B	colon carcinoma	B	SR	B
3	69	female	430	septic shock	B	ASVD	A	SR	B
4	59	male	490	heart failure	A	ASVD	A	SR	B
5	63	male	380	cerebral death	B	liver cirrhosis	B	SR	B
6	77	male	580	heart failure	A	ASVD	A	SR	B
7	77	female	450	respiratory failure	B	ASVD	A	AF	A
8	77	male	490	heart failure	A	ASVD	A	SR	B
9	69	female	430	cardiogenic shock	A	ASVD	A	AF	A
10	76	male	540	heart failure	A	ASVD	A	SR	B
11	44	male	280	cerebral death	B	arterial hypertension	A	SR	B
12	76	female	360	hemorrhagic shock	B	gastric peptic ulcer	B	SR	B
13	54	male	610	heart failure	A	ASVD	A	SR	B
14	39	female	290	hemorrhagic shock	B	chronic alcoholism	B	SR	B
15	70	male	310	respiratory failure	B	ASVD	A	SR	B
16	54	male	460	heart failure	A	liver cirrhosis	B	AF	A
17	57	female	420	cerebral death	B	cerebral vascular malformation	B	SR	B
18	52	female	370	respiratory failure	B	eating disorder	B	AF	A
19	77	male	570	cardiorespiratory insufficiency	A	ASVD	A	SR	B
20	77	female	590	hemorrhagic shock	B	ASVD	A	SR	B
21	77	female	620	heart failure	A	ASVD	A	AF	A
22	46	female	320	cerebral death	B	non-cerebral vascular malformation	A	SR	B
23	80	male	410	urosepsis	B	ASVD	A	AF	A
24	52	male	570	bronchopneumonia	B	laryngeal carcinoma	B	SR	B

ASVD, atherosclerotic vascular disease; CVS, cardiovascular; AF, atrial fibrillation; SR, sinus rhythm

Table 1b
Division of subjects

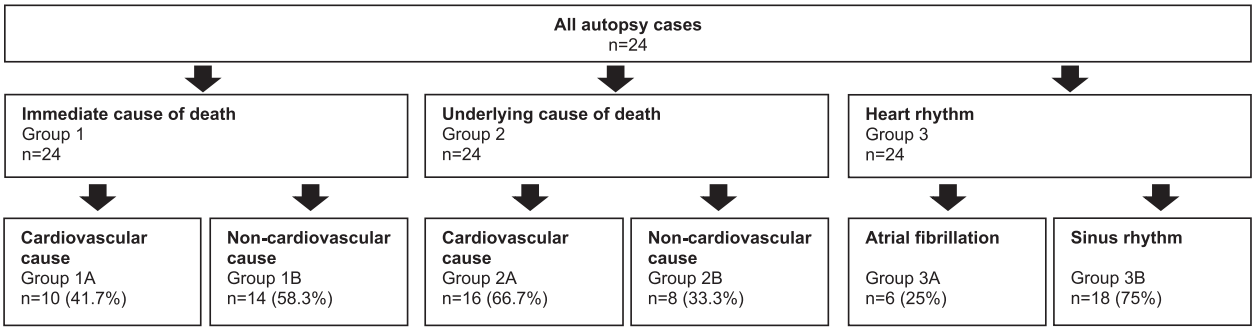

subjects had sinus rhythm (group 3B). No cases of sudden cardiac death were included as they were subjects of forensic autopsies in the Czech Republic at the time of material collection. Sudden cardiac death was not present in the one included case of myocardial infarction. All clinical data used in this study were obtained from referrals to autopsy. Further details on atrial fibrillation diagnosis were not available. More details on subjects' characteristics and group division are shown in Table 1.

2.3. Immunohistochemistry

Five-micrometer-thick serial sections were cut. The primary antibodies were anti-tyrosine hydroxylase (TH; dilution 1:100, AB152, Chemicon, Merck KGaA, Darmstadt, Germany) to visualize sympathetic nerves and ganglia, anti-choline acetyltransferase (CHAT; dilution 1:300, AB143, Chemicon, Merck KGaA, Darmstadt, Germany) to identify parasympathetic nerves and ganglia, and growth-associated protein 43 (GAP43; dilution 1:100, AB5220, Chemicon, Merck KGaA, Darmstadt, Germany) as a neural growth marker. The immunohistochemical staining was done using the Ventana Automatic System (Ventana Medical Systems, Tucson, AZ, USA).

2.4. Morphological analysis

The whole slides were digitized at 40x magnification by the NanoZoomer-XR scanner (Hamamatsu Photonics, Hamamatsu, Japan). Open-source software for bioimage analysis (QuPath, Queens University, Belfast, Northern Ireland [24]) was used for morphometrical analysis. Areas of the whole section (WS), myocardial sleeves (MS), and surrounding fibro-fatty tissue (FFT) outside the sleeve (mm^2) were measured in all caval vein samples.

The nerve area (μm^2) was separately examined by manual delimiting of positively stained nerves and ganglia with parallel eye control of the structure histological pattern, using 20x magnification. The nerve density ($\mu m^2/mm^2$) was calculated to determine the autonomic nerve distribution in all (whole section, myocardial sleeves, fibro-fatty tissue) areas. Measurements were performed separately for TH-stained, CHAT-stained, and GAP43-stained samples.

2.5. Statistical analysis

Quantitative variables were listed as the mean and standard deviation (SD) of the mean. Categoric variables were stated as the count and percentage. Statistical analysis was performed with the

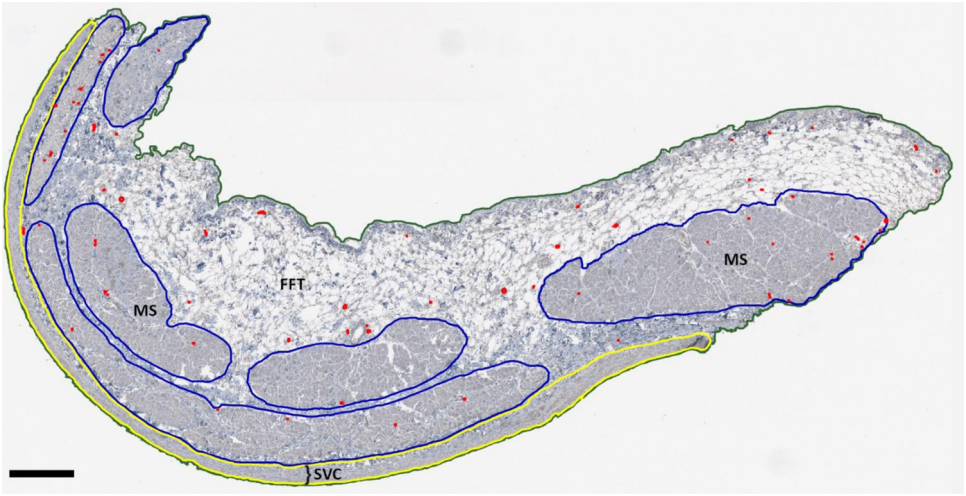

Fig. 2. Low-power histological section. The WS (marked by green line) of SVC (marked by yellow line) with myocardial MS (marked by blue line) and the surrounding FFT outside the myocardial sleeves. Positive nerves and ganglia (marked in red) were found in both MS and FFT regions (TH stain, bar=400 μm). (WS – whole slide, SVC – superior vena cava, MS – myocardial sleeve, FFT – fibro-fatty tissue, TH – tyrosine hydroxylase) (Color version of the figure is available online.) (For interpretation of the references to color in this figure, the reader is referred to the web version of this article.)

Statistical Package for the Social Sciences version 24.0 (SPSS Inc., Chicago, IL, USA). The Mann–Whitney test was used for continuous variables, and the chi-square test was used for categoric analysis. A 2-tailed *P*-value of $< .05$ was considered significant.

3. Results

3.1. Study groups characteristics

Each group included caval veins from all 24 subjects and differences between the subgroups (A vs. B) were studied. Most subjects (87.5%) belonging to the group with the documented underlying cardiovascular cause of death (group 2A) were diagnosed with systemic atherosclerosis. The mean age of group 2A was significantly higher than those with the documented underlying non-cardiovascular cause of death (group 2B) (69.2±11.9 years ± SD, vs. 57.5±11.2 years ± SD, $P = .016$). No statistical differences occurred between the other studied subgroups (group 1A vs. 1B; group 3A vs. 3B) in sex, heart weight, and age.

3.2. Caval vein myocardial sleeves and autonomic nerves

Altogether, 197 samples of CV tissue from 24 autopsies (24 superior and 24 inferior caval veins) were collected and included in this study. Myocardial sleeves were found in 42 out of 48 (87.5%) caval veins. The myocardial sleeves extended from the right atrium into the proximal part of the CV wall and were surrounded by variously abundant FFT (Fig. 2). Nerves and ganglia were identified both in MS and FFT (Fig. 3). TH and CHAT antibodies' immunoreactivity in the nerve structures confirmed the presence of autonomic nerves. Neural growth was confirmed by GAP43 positivity. The identified nerves were variably sized and shaped, some accompanied vascular structures. So-called intermediate nerves, which contained both sympathetic and parasympathetic filaments and thus partially stained with both antibodies, were considered according to the predominant immunoreactivity.

3.3. Superior vena cava area

3.3.1. Nerve densities

All nerve densities and areas are represented in mean ± SD. The overall SVC mean nerve density of TH-positive nerves in the WS, MS, and FFT was 2007.41±1700.83 $\mu m^2/mm^2$, 1266.88±1537.86 $\mu m^2/mm^2$, and 2126.25±1736.51 $\mu m^2/mm^2$, respectively. The nerve density of CHAT-positive nerve fibers in the WS, MS, and FFT was 155.79±367.59 $\mu m^2/mm^2$, 75.75±186.26 $\mu m^2/mm^2$, and 190.17±431.12 $\mu m^2/mm^2$, respectively. The GAP43-positive nerves' density in the WS, MS, and FFT was 2235.95±2063.81 $\mu m^2/mm^2$, 1300.79±1549.61 $\mu m^2/mm^2$, and 2462.18±2237.75 $\mu m^2/mm^2$, respectively.

The mean TH-, CHAT-, and GAP43-positive nerve densities between studied subjects divided into groups according to causes of death are shown in Table 2. Statistically significant differences were found between subjects with the documented underlying cardiovascular vs. non-cardiovascular cause of death (group 2A vs. 2B). TH-positive nerve density of the MS was significantly decreased in group 2A vs. group 2B (704.81±1016.41 $\mu m^2/mm^2$ vs. 2391.01±1841.37 $\mu m^2/mm^2$; $P = .008$) (Fig. 4 A, B). Moreover, the mean GAP43-positive nerve density in the MS was significantly lower in group 2A vs. group 2B (884.74±1240.16 $\mu m^2/mm^2$ vs. 2132.89±1845.89 $\mu m^2/mm^2$; $P = .040$) (Fig. 4 E, F).

No differences in nerve densities were found among subjects deceased due to immediate cardiovascular (group 1A) and non-cardiovascular cause of death (group 1B). Moreover, there were no differences in nerve densities found between subjects with a history of atrial fibrillation (group 3A) vs. sinus rhythm (group 3B) in SVC (Tab. 2). The nerve densities measured in SVC are graphically represented in Fig. 5.

3.3.2. Nerve areas

The mean nerve area of TH-positive nerves in the SVC WS, MS, and FFT was 425085.17±409831.99 μm^2, 83254.56±145078.88 μm^2, and 341830.61±368902.20 μm^2, respectively. The CHAT-positive nerves' area in the WS, MS, and FFT was 26443.47±53471.39 μm^2, 608.17±1155.34 μm^2, and 25829.88±53377.31 μm^2, respectively. Similarly, the mean nerve area of GAP43-positive nerve fibers in the SVC WS, MS, and FFT was 470147.38±485693.08 μm^2, 83121.50±143174.27 μm^2, and 387238.59±440156.57 μm^2, respectively.

3.4. Inferior vena cava area

3.4.1. Nerve densities

The overall IVC nerve density of TH-positive nerves in the WS, MS, and FFT was 1737.05±2294.43 $\mu m^2/mm^2$, 933.33±1420.07

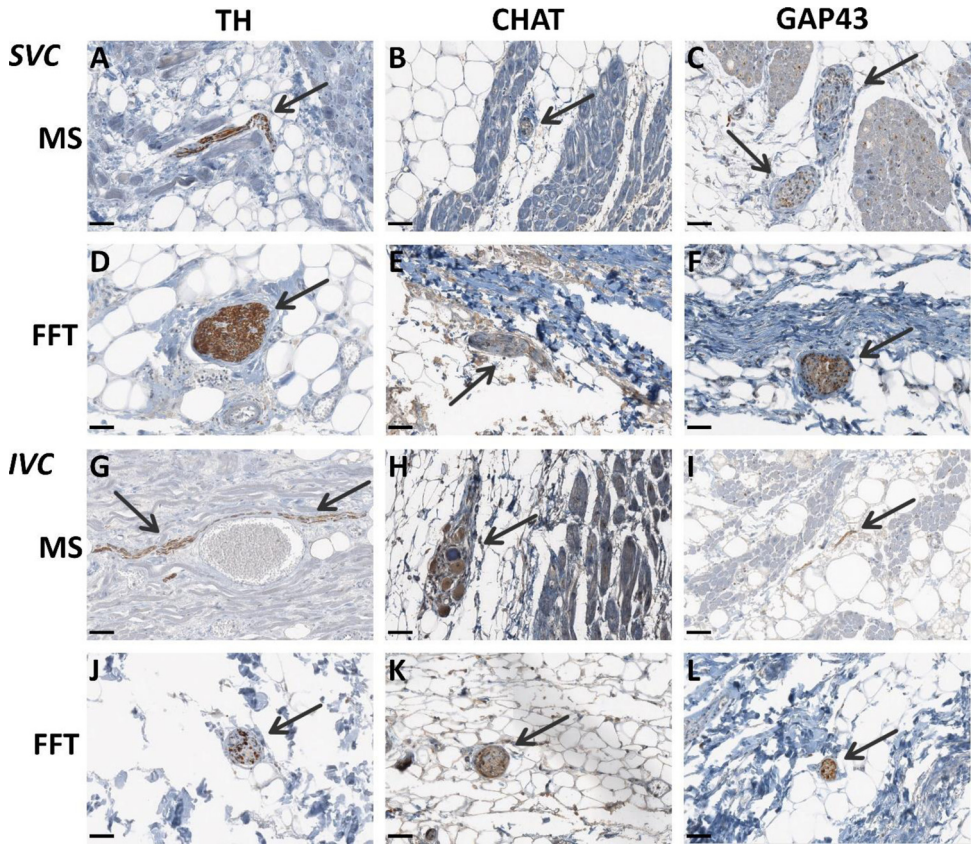

Fig. 3. Representative histological sections of autonomic nerves and ganglia. (A-F) superior vena cava (SVC); (G-L) inferior vena cava (IVC). (A) a longitudinal section of TH-positive nerve (arrow) in the middle of the MS with profound fatty replacement; (B) a transverse section of CHAT-positive nerve (arrow) in the MS with large fatty replacement; (C) a tangential section of GAP43-positive nerve (arrows) in the middle of myocardial bundles in the MS surrounded by adipose tissue; (D) a transverse section of TH positive nerve (arrow) close to several vascular structures surrounded by FFT outside MS; (E) a longitudinal section of CHAT-positive nerve (arrow) adjacent to the fibrous area and adipose tissue; (F) a transverse section of GAP43-positive nerve (arrow) adjacent to thick fibrosis and adipose tissue; (G) a longitudinal TH-positive nerve stain (arrows) perpendicular to a dilated vein surrounded by waved cardiomyocytes in the MS; (H) a parasympathetic ganglion (arrow) within the MS, surrounded by mildly hypertrophic cardiomyocytes and fat replacement; (I) a longitudinal section of two nerves positive for GAP43 (arrow) in the MS with partial fatty replacement; (J) a transverse section of an intermediate nerve (arrow) predominantly stained for TH in the FFT; (K) a CHAT-positive nerve (arrow) surrounded by fatty tissue in FFT area; (L) a nerve stain positive for GAP43 (arrow) in the adipose tissue between two fibrotic areas. (A-L) bar=50 µm. (MS – myocardial sleeve, FFT – fibro-fatty tissue, TH – tyrosine hydroxylase detecting sympathetic nerve tissue, CHAT – choline acetyltransferase detecting parasympathetic nerve tissue, GAP43 – growth-associated protein 43 detecting neural growth).

Table 2
Vena cava superior – Autonomic nerve densities related to cause of death and heart rhythm

Studied marker	Area	Immediate cardiovascular death (group 1A)	Immediate non-cardiovascular death (group 1B)	Underlying cardiovascular death (group 2A)	Underlying non-cardiovascular death (group 2B)	Atrial fibrillation (group 3A)	Sinus rhythm (group 3B)
TH	WS	2249.79 ±1872.68	1834.28 ±1616.39	1923.07 ±1791.6	2176.1 ±1605.61	2972.22 ±2110.35	1685.81 ±1471.69
	MS	1374.79 ±2078.41	1189.8 ±1085.48	**704.81 ±1016.41***	**2391.01 ±1841.37***	1753.08 ±2633.39	1104.81 ±1024.13
	FFT	2334.68 ±1845.09	1977.36 ±1709.06	2010.34 ±1845.87	2358.06 ±1585.75	2840.65 ±2167.42	1888.11 ±1567.76
CHAT	WS	205.08 ±481.43	120.58 ±274.6	117.16 ±266.44	233.05 ±530.68	281.7 ±616.7	113.82 ±251.98
	MS	71.26 ±217.16	78.95 ±169.42	112.56 ±221.02	2.11 ±3.92	116.32 ±280.65	62.22 ±151.65
	FFT	247.52 ±590.83	149.21 ±287.81	122.27 ±276.75	325.95 ±644.19	338.25 ±760.26	140.81 ±266.74
GAP43	WS	2758.45 ±2456	1862.73 ±1731.97	2049.38 ±2011.15	2609.08 ±2255.87	3099.53 ±2596.51	1948.09 ±1851.68
	MS	1577.69 ±1987.99	1103 ±1187.98	**884.74 ±1240.16#**	**2132.89 ±1845.89#**	1737.79 ±2438.77	1155.12 ±1187.29
	FFT	3064.62 ±2570.65	2031.86 ±1950.89	2227.69 ±2105.69	2931.15 ±2564.2	3095.82 ±2869.69	2250.96 ±2040.56

Values are mean densities in $\mu m^2/mm^2$ ± SD.
WS, whole slide; MS, myocardial sleeve; FFT, fibro-fatty tissue; TH, tyrosine hydroxylase; CHAT, choline acetyltransferase; GAP43, growth-associated protein 43.
* $P = .008$
# $P = .040$.

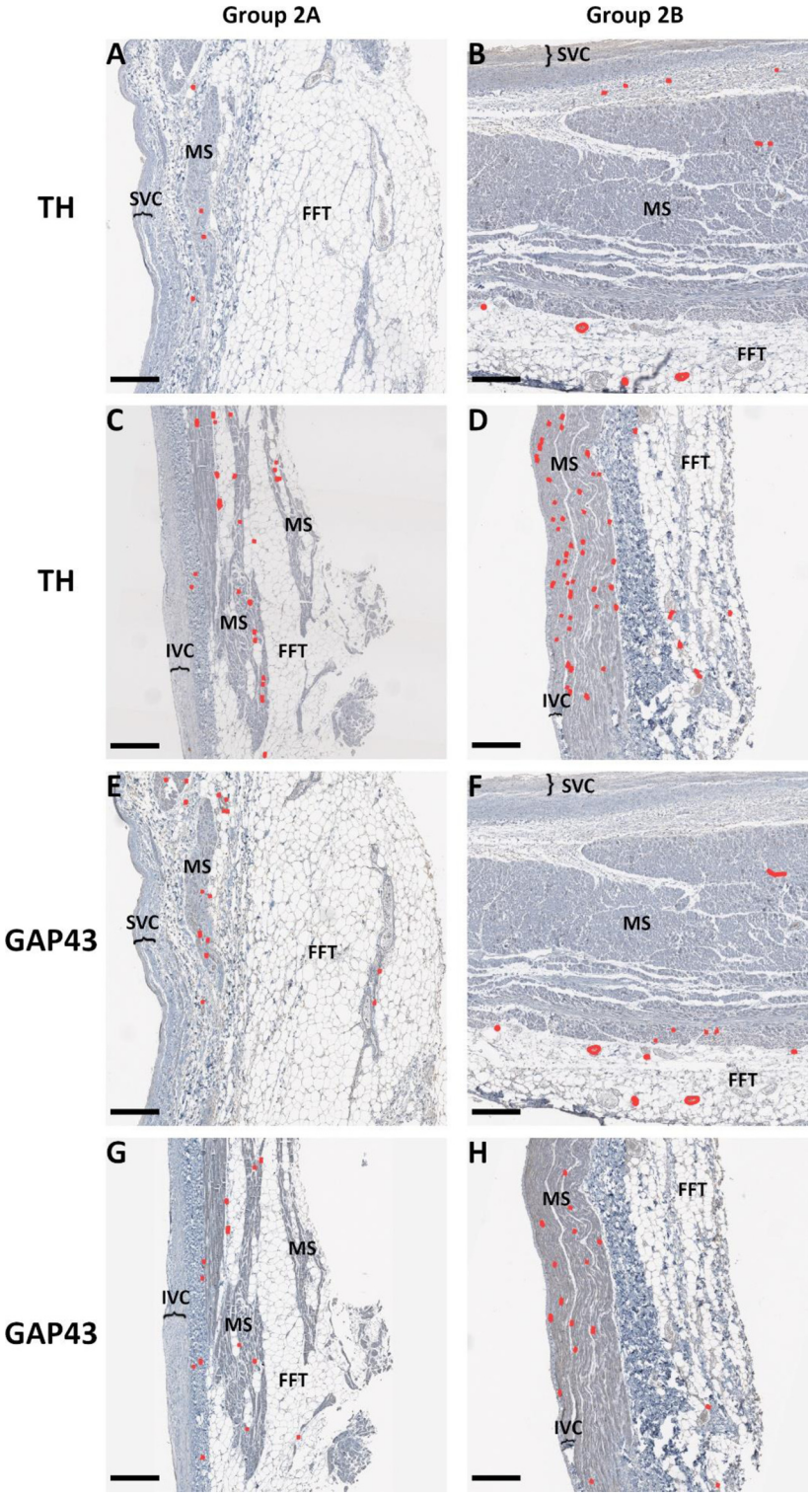

Fig. 4. Morphological comparison of low-power histological sections of superior (SVC) and inferior vena cava (IVC) between subjects with the documented underlying cardiovascular (group 2A) and non-cardiovascular cause of death (group 2B). Positive nerves and ganglia are defined in red and were found in both MS and FFT regions. (A) a thin discontinuous mildly fibrotic MS next to SVC. Abundant surrounding FFT outside MS consists mainly of fat, sparse fibrous area, and several larger vessels. Only a few TH-positive nerves were detected both in MS and in the adjacent fibrotic area of FFT; (B) a thick continuous MS adjacent to fibrous band next to SVC and surrounded by adipose FFT. TH positive nerves are mainly in FFT area, but also in MS to a lesser extent; (C) MS around IVC is discontinuous and thin. Adjacent to IVC is a fibrous band and peripherally adipose FFT. TH-positive nerves are mainly in MS and fibrous FFT; (D) longitudinally arranged myocardial fibers in continuous MS closely adjacent to IVC and surrounded by fibrous and adipose tissue of FFT. Numerous TH-positive nerves were detected in MS, less in the adipose part of FFT; (E) SVC area corresponding to the area in figure A with GAP43-positive nerves found in MS and surrounding FFT. Some nerves accompany vascular structures on the right side of the figure; (F) SVC area corresponding to the same area as in figure B, GAP43-positive nerves were found both in MS and in the FFT; (G) IVC area corresponding to the area in figure C with GAP43-positive nerves detected mainly in MS and in fibrous part of FFT; (H) IVC area corresponding to the area in figure D with many GAP43-positive nerves found in longitudinally arranged myocytes of MS; (A-H) bar=400 μm. (SVC – superior vena cava, IVC – inferior vena cava, MS – myocardial sleeve, FFT – fibro-fatty tissue, TH – tyrosine hydroxylase, GAP43 – growth-associated protein 43). (For interpretation of the references to color in this figure, the reader is referred to the web version of this article.)

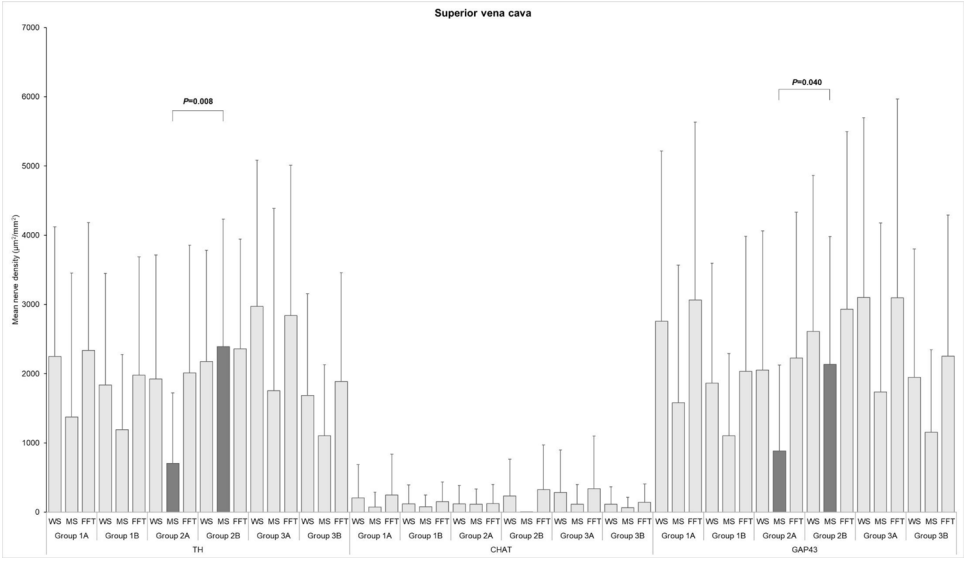

Fig. 5. Superior vena cava: Comparison of autonomic nerve densities ($\mu m^2/mm^2$) between subjects with the documented immediate cardiovascular (group 1A) and non-cardiovascular cause of death (group 1B), underlying cardiovascular (group 2A) and non-cardiovascular cause of death (group 2B), and subjects with a medical history of atrial fibrillation (group 3A) and sinus rhythm (group 3B). A statistically significant difference ($P < .05$) is highlighted in TH- and GAP43-positive nerves in MS between groups 2A and 2B. WS-whole section, MS-myocardial sleeves, FFT-surrounding fibro-fatty tissue outside the sleeve, TH-tyrosine hydroxylase, CHAT-choline acetyltransferase, GAP43-growth-associated protein 43.

Table 3
Vena cava inferior – Autonomic nerve densities related to cause of death and heart rhythm

Studied marker	Area	Immediate cardiovascular death (group 1A)	Immediate non-cardiovascular death (group 1B)	Underlying cardiovascular death (group 2A)	Underlying non-cardiovascular death (group 2B)	Atrial fibrillation (group 3A)	Sinus rhythm (group 3B)
TH	WS	1401.41 ±1014.81	1976.79 ±2907.3	1904.39 ±2620.74	1402.37 ±1545.15	2863.76 ±3954.82	1361.47 ±1387.38
	MS	953.01 ±1042.93	919.26 ±1677.58	717.23 ±887.31	1365.51 ±2149.1	235.07 ±425.69	1166.08 ±1563.84
	FFT	1372.08 ±1034.68	1847.05 ±2918.94	1955.05 ±2754.47	1037.33 ±698.49	2986.4 ±4154.55	1203.39 ±1114.25
CHAT	WS	244.89 ±514.99	909.3 ±2883.08	892.17 ±2703.7	113.04 ±137.48	2152.28 ±4338.88	125.85 ±155.62
	MS	180.8 ±532.9	374.22 ±894.76	256.18 ±666.86	368.53 ±959.47	648.59 ±1017.33	175.31 ±641.65
	FFT	342.97 ±638.69	975.39 ±2989.38	997.72 ±2804.78	140.21 ±190.56	2229.7 ±4512.26	205.94 ±338.26
GAP43	WS	1757.65 ±1542.48	2252.36 ±3143.73	2284.76 ±2929.82	1569.17 ±1683.17	3623.76 ±4277.01	1520.38 ±1532.92
	MS	593.58 ±507.97	1337.34 ±1747.69	661.21 ±839.51	1759.9 ±2008.8	990.17 ±1315.18	1039.86 ±1467.23
	FFT	2033.75 ±1790.54	2423.62 ±3234.29	2596.25 ±3080.38	1591.02 ±1603.96	3762.89 ±4442.21	1760.6 ±1698.12

Values are mean densities in $\mu m^2/mm^2 \pm$ SD.
WS, whole slide; MS, myocardial sleeve; FFT, fibro-fatty tissue; TH, tyrosine hydroxylase; CHAT, choline acetyltransferase; GAP43, growth-associated protein 43.

$\mu m^2/mm^2$, and 1649.14±2300.41 $\mu m^2/mm^2$, respectively. The mean nerve density of CHAT-positive nerve fibers in the IVC WS, MS, and FFT was 632.46±2216.74 $\mu m^2/mm^2$, 293.63±757.05 $\mu m^2/mm^2$, and 711.88±2304.79 $\mu m^2/mm^2$, respectively. The nerve density of GAP43-positive nerves in the IVC WS, MS, and FFT was 2046.23±2564.99 $\mu m^2/mm^2$, 1027.44±1402.74 $\mu m^2/mm^2$, and 2261.17±2684.32 $\mu m^2/mm^2$, respectively.

There were no differences in the autonomic nerve densities and the GAP43-positive nerve densities within the WS, MS, and FFT areas surrounding IVC between the studied groups (Fig. 4 C, D, H, G). Detailed nerve density data concerning causes of death and heart rhythm history are shown in Table 3 and Fig. 6.

3.4.2. Nerve areas

The mean nerve area of TH-positive nerves in the WS, MS, and FFT areas surrounding IVC was 217820.33±259007.41 μm^2, 69810.73±135612.05 μm^2, and 147734.00±236825.87 μm^2, respectively. The nerve area of CHAT-positive nerve fibers in the WS, MS, and FFT was 69826.00±228817.15 μm^2, 3139.64±6762.70 μm^2, and 66210.03±226594.79 μm^2, respectively. The nerve area of GAP43-positive nerves in the IVC WS, MS, and FFT was 246950.03±271833.54 μm^2, 50594.11±85487.54 μm^2, and 196355.92±259628.12 μm^2, respectively.

4. Discussion

4.1. Original findings

The most important finding was the statistically significant association between the decrease of TH- and GAP43-positive nerve densities in the SVC myocardial sleeves and the underlying cardiovascular cause of death ($P < .05$). Of note, the mean age of subjects with the documented underlying cardiovascular cause of

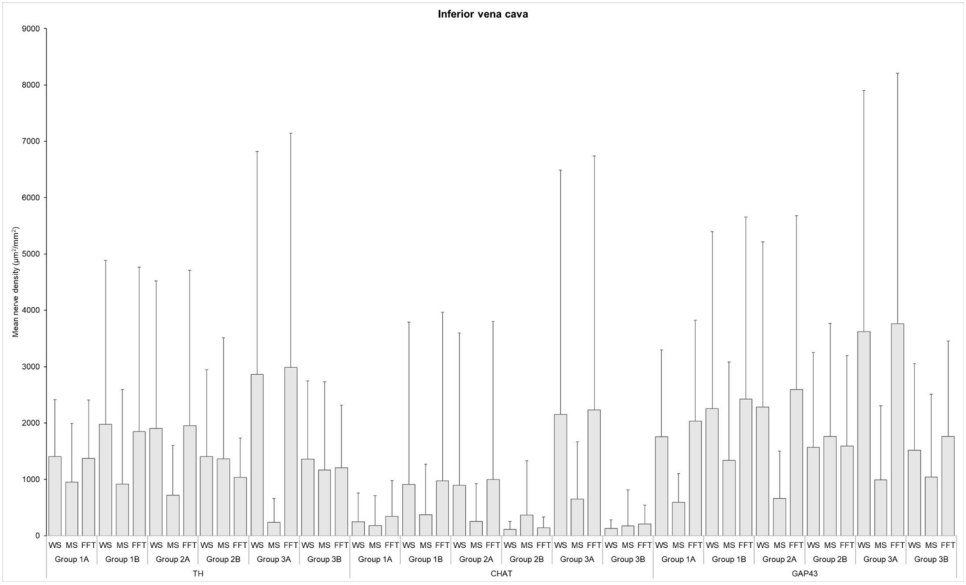

Fig. 6. Inferior vena cava: Comparison of autonomic nerve densities ($\mu m^2/mm^2$) between subjects with the documented immediate cardiovascular (group 1A) and non-cardiovascular cause of death (group 1B), underlying cardiovascular (group 2A) and non-cardiovascular cause of death (group 2B), and subjects with a medical history of atrial fibrillation (group 3A) and sinus rhythm (group 3B). WS-whole section, MS-myocardial sleeves, FFT-surrounding fibro-fatty tissue outside the sleeve, TH-tyrosine hydroxylase, CHAT-choline acetyltransferase, GAP43-growth-associated protein 43.

death (group 2A) was significantly higher than those with the documented underlying non-cardiovascular cause of death (group 2B). The nerve density of the whole area and surrounding fibro-fatty tissue of the SVC did not show a difference in nerve densities between the studied groups. There was no difference found in nerve densities in the SVC and IVC between subjects with documented immediate cardiovascular (group 1A) and non-cardiovascular cause of death (group 1B), and between subjects with a history of atrial fibrillation (group 3A) and sinus rhythm (group 3B).

We evaluated the nerve density of human superior and inferior caval veins with immunohistochemical and morphometrical analysis. The autopsy material is unique providing the possibility to study large topographical areas and whole anatomical compartments. We assessed the differences in autonomic innervation and neural growth between subjects with the documented underlying cardiovascular and non-cardiovascular cause of death, immediate cardiovascular and non-cardiovascular cause of death, and history of atrial fibrillation. The nerves and ganglia of various sizes and shapes were located both in MS and FFT. Some of the nerves accompanied vascular structures.

4.2. The significance of myocardial sleeves around caval veins and their denervation

According to the literature, there are differences between SVC and IVC in terms of electrical and mechanical activity. The atrial electrical activity was found extending for 2 to 4 cm into SVC, but not into IVC [25]. Similarly, contraction only in the SVC was reported by Arita et al [26]. On the other hand, previous studies suggested possible contraction of both SVC and IVC [1,27]. They described histologically that myocardial sleeves from the right atrium extend into SVC an average of 13.7 mm, with a mean thickness of 1.2 mm, and into IVC an average of 14.6 mm, with a mean thickness of 1.2 mm [1]. The physiologic significance of these findings is that the myocardial sleeves are contractile structures that create a functional valve for the prevention of backflow and facilitate the ejection of blood into the right atrium during the cardiac cycle [26–28].

Our observations demonstrate sympathetic denervation and decreased neuronal growth in the myocardial sleeves around SVC in patients with the documented underlying cardiovascular cause of death. These changes could alter valve function and contribute to hemodynamic impairment. However, the ANS innervation and nerve growth in the myocardial sleeves around IVC were not affected when compared to patients with the documented underlying cause of death other than cardiovascular.

4.3. Abnormalities of the autonomic innervation in heart failure

The importance of ANS regulation in the cardiovascular system has been well established in various physiological and pathological conditions [10]. We found that sympathetic denervation and decreased neural growth are associated with cardiovascular mortality. Changes in autonomic innervation are also prominent in heart failure, playing an important role in mortality and poor prognosis of this condition. In agreement with the present results on the human CV myocardial sleeves, previous studies have demonstrated that despite increased sympathetic activity in chronic heart failure, characterized by an elevated plasma concentration and release of cardiac catecholamines, the density of the sympathetic nerves is reduced [16,17,29,30]. Siltanen et al [17] showed that sympathetic innervation, measured by TH activity in the human auricular appendages, was decreased in chronic heart failure compared to subjects with ischemic heart disease. Himura et al [16] found severe sympathetic denervation in dogs with chronic heart failure. The pathophysiology of the loss of cardiac sympathetic nerve density in heart failure can be explained by decreased expression of nerve growth factor [31], and oxidative stress [32].

In our study, a decrease in GAP43-positive nerve density in myocardial sleeves around SVC was significantly related to underlying cardiovascular cause of death. A decrease in neural growth in chronic heart failure was demonstrated by Cha et al [15], who observed a heterogeneous decrease in the atrial GAP43-positive nerve density in dogs with pacing-induced chronic heart failure. Interestingly, by preventing the decrease in GAP43-positive nerve density using pharmacologic intervention, they reduced adverse cardiac structural remodeling.

4.4. Myocardial ischemia and sympathetic denervation

It was shown that sympathetic nerves are damaged and reduced in infarcted myocardium [33]. Similarly, a previous study reported that sympathetic nervous tissue is more sensitive to ischemia than myocardial tissue and that coronary artery disease without previous myocardial infarction causes sympathetic denervation of myocardial tissue [34]. In a study by Simula et al [35], sympathetic nerve terminals were impaired even in the early stages of coronary atherosclerosis. Of note, 87.5% of the subjects belonging to group 2A were diagnosed with systemic atherosclerosis in our series. Although only one of these subjects died of myocardial infarction, usually small ischemic changes in the myocardium can be seen in autopsy hearts of subjects with coronary atherosclerosis. Reduction in histological sympathetic nerve density and compensatory increased neuronal sprouting was also demonstrated in hibernating porcine myocardium as a response to repetitive ischemia in the absence of infarction [36]. However, in the atria, the TH- and GAP43-positive nerve density was higher in dogs with chronic left ventricular myocardial infarction [18].

The clinical relevance of these facts consists in the excessive response of the denervated myocardium to sympathetic stimulation [37]. Thus, heterogeneous sympathetic denervation could be one of the sources that increase vulnerability to arrhythmias and sudden cardiac death during myocardial ischemia. Furthermore, alterations in ANS lead to the progression of atherosclerosis via dysregulation of inflammatory cytokines, neurotransmitters, and endothelial dysfunction [38,39], which may further promote myocardial ischemia. These findings provide support for using imaging methods to evaluate myocardial sympathetic denervation as prognostic information to assess cardiac mortality [40].

4.5. Age-related neurodegeneration

Aging, as the most significant risk factor for cardiovascular mortality [41], contributes to structural and functional remodeling of the myocardium [42]. Several studies have demonstrated that gradual degeneration of sympathetic nerves and decrease in TH-positive nerve density within the myocardium is related to aging [43–45]. In our study, subjects in group 2A were significantly older than those in group 2B. Although these findings are consistent with the previous studies [43–45], denervation of myocardial sleeves around SVC may be explained by age-related neurodegeneration. Our results suggest that aging may be associated with myocardial susceptibility to arrhythmias and eventually leads to increased mortality.

4.6. Caval veins myocardial sleeves and atrial fibrillation

A previous canine study compared the cholinergic nerve densities in different supraventricular regions of the heart, including SVC [9]. Interestingly, they did not find differences between SVC and other parts of the heart including pulmonary veins. On the other hand, the cholinergic nerve densities were higher in both the left and right atrial appendages, left and right atria, compared to SVC. These findings suggest heterogeneous parasympathetic innervation within the myocardium of the supraventricular regions of the heart. Since SVC and pulmonary vein cholinergic nerve densities did not differ, we can assume the SVC has similar arrhythmogenic potential as pulmonary veins. Nevertheless, we did not find any correlation in nerve densities in subjects belonging to group 3A in comparison to the subjects in group 3B. Autopsy studies have however limitations and data about the medical history of heart rhythm may be incomplete.

In contrast to studies supporting the arrhythmogenic effect of increased atrial ANS innervation and nerve sprouting [19–22], however, other previous studies do not support this hypothesis [46–48]. We found that ANS innervation and neural growth in SVC and IVC myocardial sleeves were not associated with the presence of atrial fibrillation.

4.7. Limitations of the study

Clinical data used in our study were obtained only from the referrals to the autopsy, therefore, some information may be incomplete. No details were available about the pharmacologic therapy (e.g. beta-blockers), which may influence the autonomic innervation pattern [49]. Older population with underlying cardiovascular cause of death was overrepresented as it is in hospital autopsies. The conclusions may be limited due to the small number of autopsies included in the study. The study series does not include any cases of sudden cardiac death. Each of the three studied groups included all 24 subjects and differences were assessed between the subgroups (A vs. B).

5. Conclusions

In conclusion, denervation of SVC myocardial sleeves caused by various factors, including aging, may serve as one of the possible mechanisms of increased mortality in patients suffering from cardiovascular diseases. Furthermore, no association in the autonomic nerve density was found between subjects with a history of atrial fibrillation and sinus rhythm. In further research, more focus on the pathophysiology of denervation and its degree in different parts of the heart is therefore suggested.

Declaration of interests

The authors declare that they have no known competing financial interests or personal relationships that could have appeared to influence the work reported in this paper.

Acknowledgments

This study was funded by grants from the Competitive Research Funding of the Pirkanmaa Hospital District (to IK, AM, TP), Tampere University Hospital Support Foundation (to IK), Aarne Koskelo Foundation (to IK), Emil Aaltonen Foundation (to IK), and the Research Foundation for Laboratory Medicine (to DD). The results were presented as a poster and awarded as the “Highly commended poster presentation” at the 9th Biennial Meeting of the Association for European Cardiovascular Pathology in Cambridge, UK, September 16th-18, 2021. The authors thank Eini Eskola and Sari Toivola for their expert laboratory work.

References

[1] Kholová I, Kautzner J. Morphology of atrial myocardial extensions into human caval veins: a postmortem study in patients with and without atrial fibrillation. Circulation 2004;110:483–8. doi:10.1161/01.CIR.0000137117.87589.88.
[2] Tsai CF, Tai CT, Hsieh MH, Lin WS, Yu WC, Ueng KC, et al. Initiation of atrial fibrillation by ectopic beats originating from the superior vena cava: Electrophysiological characteristics and results of radiofrequency ablation. Circulation 2000;102:67–74. doi:10.1161/01.CIR.102.1.67.
[3] Scavée C, Jaïs P, Weerasooriya R, Haïssaguerre M. The inferior vena cava: an exceptional source of atrial fibrillation. J Cardiovasc Electrophysiol 2003;14:659–62. doi:10.1046/j.1540-8167.2003.03027.x.
[4] Desimone CV, Noheria A, Lachman N, Edwards WD, Gami AS, Maleszewski JJ, et al. Myocardium of the superior vena cava, coronary sinus, vein of marshall, and the pulmonary vein ostia: Gross anatomic studies in 620 hearts. J Cardiovasc Electrophysiol 2012;23:1304–9. doi:10.1111/j.1540-8167.2012.02403.x.
[5] Yeh HI, Lai YJ, Lee SH, Lee YN, Ko YS, Chen SA, et al. Heterogeneity of myocardial sleeve morphology and gap junctions in canine superior vena cava. Circulation 2001;104:3152–7. doi:10.1161/hc5001.100836.
[6] Chen YJ, Chen YC, Yeh HI, Lin CI, Chen SA. Electrophysiology and arrhythmogenic activity of single cardiomyocytes from canine superior vena cava. Circulation 2002;105:2679–85. doi:10.1161/01.CIR.0000016822.96362.26.

[7] Saito T, Waki K, Becker A. Left atrial myocardial extension onto pulmonary veins in humans: anatomic observations relevant for atrial arrhythmias. J Cardiovasc Electrophysiol 2000;11:888–94. doi:10.1111/J.1540-8167.2000.TB00068.X.
[8] Kholová I, Kautzner J. Anatomic characteristics of extensions of atrial myocardium into the pulmonary veins in subjects with and without atrial fibrillation. PACE - Pacing. Clin Electrophysiol 2003;26:1348–55. doi:10.1046/j.1460-9592.2003.t01-1-00193.x.
[9] Li Z, Zhao QY, Huang H, Yang B, Jiang H, Huang CX. Differential densities of cholinergic nerves in canine supraventricular regions of hearts. J Cardiol 2013;61:232–6. doi:10.1016/j.jjcc.2012.12.003.
[10] Durães Campos I, Pinto V, Sousa N, Pereira VH. A brain within the heart: a review on the intracardiac nervous system. J Mol Cell Cardiol 2018;119:1–9. doi:10.1016/j.yjmcc.2018.04.005.
[11] Florea VG, Cohn JN. The autonomic nervous system and heart failure. Circ Res 2014;114:1815–26. doi:10.1161/CIRCRESAHA.114.302589.
[12] Wake E, Brack K. Characterization of the intrinsic cardiac nervous system. Auton Neurosci Basic Clin 2016;199:3–16. doi:10.1016/j.autneu.2016.08.006.
[13] Shen MJ, Zipes DP. Role of the autonomic nervous system in modulating cardiac arrhythmias. Circ Res 2014;114:1004–21. doi:10.1161/CIRCRESAHA.113.302549.
[14] Fukuda K, Kanazawa H, Aizawa Y, Ardell JL, Shivkumar K. Cardiac innervation and sudden cardiac death. Circ Res 2015;116:2005–19. doi:10.1161/CIRCRESAHA.116.304679.
[15] Cha YM, Redfield MM, Shah S, Shen WK, Fishbein MC, Chen PS. Effects of omapatrilat on cardiac nerve sprouting and structural remodeling in experimental congestive heart failure. Hear Rhythm 2005;2:984–90. doi:10.1016/j.hrthm.2005.05.016.
[16] Himura Y, Felten SY, Kashiki M, Lewandowski TJ, Delehanty JM, Liang CS. Cardiac noradrenergic nerve terminal abnormalities in dogs with experimental congestive heart failure. Circulation 1993;88:1299–309. doi:10.1161/01.CIR.88.3.1299.
[17] Siltanen P, Penttilä O, Merikallio E, Kyösola K, Klinge E, Pispa J. Myocardial catecholamines and their biosynthetic enzymes in various human heart diseases. Acta Med Scand 1982;211:24–33. doi:10.1111/j.0954-6820.1982.tb00357.x.
[18] Miyauchi Y, Zhou S, Okuyama Y, Miyauchi M, Hayashi H, Hamabe A, et al. Altered atrial electrical restitution and heterogeneous sympathetic hyperinnervation in hearts with chronic left ventricular myocardial infarction: Implications for atrial fibrillation. Circulation 2003;108:360–6. doi:10.1161/01.CIR.0000080327.32573.7C.
[19] Akira H, Chang CM, Zhou S, Chou CC, Yi J, Miyauchi Y, et al. Induction of Atrial Fibrillation and Nerve Sprouting by Prolonged Left Atrial Pacing in Dogs. PACE - Pacing Clin Electrophysiol 2003;26:2247–52. doi:10.1111/j.1540-8159.2003.00355.x.
[20] Swissa M, Zhou S, Tan AY, Fishbein MC, Chen PS, Chen LS. Atrial sympathetic and parasympathetic nerve sprouting and hyperinnervation induced by subthreshold electrical stimulation of the left stellate ganglion in normal dogs. Cardiovasc Pathol 2008;17:303–8. doi:10.1016/j.carpath.2007.11.003.
[21] Yu Y, Liu L, Jiang JY, Qu XF, Yu G. Parasympathetic and substance P-immunoreactive nerve denervation in atrial fibrillation models. Cardiovasc Pathol 2012;21:39–45. doi:10.1016/j.carpath.2011.01.003.
[22] Gould PA, Yii M, Mclean C, Finch S, Marshall T, Lambert GW, et al. Evidence for increased atrial sympathetic innervation in persistent human atrial fibrillation. PACE - Pacing Clin Electrophysiol 2006;29:821–9. doi:10.1111/j.1540-8159.2006.00447.x.
[23] Chang CM, Wu TJ, Zhou S, Doshi RN, Lee MH, Ohara T, et al. Nerve sprouting and sympathetic hyperinnervation in a canine model of atrial fibrillation produced by prolonged right atrial pacing. Circulation 2001;103:22–5. doi:10.1161/01.CIR.103.1.22.
[24] Bankhead P, Loughrey MB, Fernández JA, Dombrowski Y, McArt DG, Dunne PD, et al. QuPath: Open source software for digital pathology image analysis. Sci Rep 2017;7:1–7. doi:10.1038/s41598-017-17204-5.
[25] Spach M, Barr R, Jewett P. Spread of excitation from the atrium into thoracic veins in human beings and dogs. Am J Cardiol 1972;30:844–54. doi:10.1016/0002-9149(72)90009-4.
[26] Arita M, Saeki K, Tanoue M, Ito M, Yanaga T, Mashiba H. Studies on transmembrane action potentials and mechanical responses of the venae cavae and atria of the rabbit. Jpn J Physiol 1966;16:462–80. doi:10.2170/JJPHYSIOL.16.462.
[27] Hashizume H, Ushiki T, Abe K. A histological study of the cardiac muscle of the human superior and inferior venae cavae. Arch Histol Cytol 1995;58:457–64. doi:10.1679/AOHC.58.457.
[28] Nathan H, Gloobe H. Myocardial atrio-venous junctions and extensions (sleeves) over the pulmonary and caval veins. Anatomical observations in various mammals. Thorax 1970;25:317–24. doi:10.1136/thx.25.3.317.
[29] Wang K, Zhu Z-F, Chi R-F, Li Q, Yang Z-J, Jie X, et al. The NADPH oxidase inhibitor apocynin improves cardiac sympathetic nerve terminal innervation and function in heart failure. Exp Physiol 2019;104:1638–49. doi:10.1113/EP087552.
[30] Kreusser MM, Buss SJ, Krebs J, Kinscherf R, Metz J, Katus HA, et al. Differential expression of cardiac neurotrophic factors and sympathetic nerve ending abnormalities within the failing heart. J Mol Cell Cardiol 2008;44:380–7. doi:10.1016/J.YJMCC.2007.10.019.
[31] Kaye DM, Vaddadi G, Gruskin SL, Du X-J, Esler MD. Reduced myocardial nerve growth factor expression in human and experimental heart failure. Circ Res 2000;86. doi:10.1161/01.RES.86.7.E80.
[32] Shite J, Qin F, Mao W, Kawai H, Stevens SY, Liang C. Antioxidant vitamins attenuate oxidative stress and cardiac dysfunction in tachycardia-induced cardiomyopathy. J Am Coll Cardiol 2001;38:1734–40. doi:10.1016/S0735-1097(01)01596-0.
[33] Ahonen A, Härkönen M, Juntunen J, Kormano M, Penttilä A. Effects of myocardial infarction on adrenergic nerves of the rat heart muscle, a histochemical study. Acta Physiol Scand 1975;93:336–44. doi:10.1111/J.1748-1716.1975.TB05822.X.
[34] Hartikainen J, Mustonen J, Kuikka J, Vanninen E, Kettunen R. Cardiac sympathetic denervation in patients with coronary artery disease without previous myocardial infarction. Am J Cardiol 1997;80:273–7. doi:10.1016/S0002-9149(97)00345-7.
[35] Simula S, Vanninen E, Viitanen L, Kareinen A, Lehto S, Pajunen P, et al. Cardiac adrenergic innervation is affected in asymptomatic subjects with very early stage of coronary artery disease. J Nucl Med 2002;43:1–7.
[36] Fernandez SF, Ovchinnikov V, Canty JM Jr, Fallavollita JA. Hibernating myocardium results in partial sympathetic denervation and nerve sprouting. Am J Physiol - Hear Circ Physiol 2013;304:H318. doi:10.1152/AJPHEART.00810.2011.
[37] Inoue H, Zipes DP. Results of sympathetic denervation in the canine heart: supersensitivity that may be arrhythmogenic. Circulation 1987;75:877–87. doi:10.1161/01.CIR.75.4.877.
[38] Sheng Y, Zhu L. The crosstalk between autonomic nervous system and blood vessels. Int J Physiol Pathophysiol Pharmacol 2018;10:17.
[39] Kadoya M, Sleep Koyama H. Autonomic nervous function and atherosclerosis. Int J Mol Sci 2019;20. doi:10.3390/IJMS20040794.
[40] Malhotra S, Fernandez SF, Fallavollita JA, Canty JM Jr. Prognostic significance of imaging myocardial sympathetic innervation. Curr Cardiol Rep 2015;17:62. doi:10.1007/S11886-015-0613-9.
[41] Mozaffarian D, Benjamin EJ, Go AS, Arnett DK, Blaha MJ, Cushman M, et al. Executive summary: heart disease and stroke statistics—2016 update. Circulation 2016;133:447–54. doi:10.1161/CIR.0000000000000366.
[42] Stuart SDF, Wang L, Woodard WR, Ng GA, Habecker BA, Ripplinger CM. Age-related changes in cardiac electrophysiology and calcium handling in response to sympathetic nerve stimulation. J Physiol 2018;596:3977–91. doi:10.1113/JP276396.
[43] Chow LTC, Chow SSM, Anderson RH, Gosling JA. Autonomic innervation of the human cardiac conduction system: changes from infancy to senility—An immunohistochemical and histochemical analysis. Anat Rec 2001;264:169–82. doi:10.1002/AR.1158.
[44] Al-Shawi R, Hafner A, Chun S, Raza S, Crutcher K, Thrasivoulou C, et al. ProNGF, Sortilin, and age-related neurodegeneration. Ann N Y Acad Sci 2007;1119:208–15. doi:10.1196/ANNALS.1404.024.
[45] Esler MD, Turner AG, Kaye DM, Thompson JM, Kingwell BA, Morris M, et al. Aging effects on human sympathetic neuronal function. 1995;268. doi:10.1152/AJPREGU.1995.268.1.R278.
[46] Deneke T, Chaar H, De Groot JR, Wilde AA, Lawo T, Mundig J, et al. Shift in the pattern of autonomic atrial innervation in subjects with persistent atrial fibrillation. Heart Rhythm 2011;8:1357–63. doi:10.1016/j.hrthm.2011.04.013.
[47] Nguyen BL, Fishbein MC, Chen LS, Chen PS, Masroor S. Histopathological substrate for chronic atrial fibrillation in humans. Heart Rhythm 2009;6:454–60. doi:10.1016/j.hrthm.2009.01.010.
[48] Yang M, Zhang S, Liang J, Tang Y, Wang X, Huang C, et al. Different effects of norepinephrine and nerve growth factor on atrial fibrillation vulnerability. J Cardiol 2019;74:460–5. doi:10.1016/j.jjcc.2019.04.009.
[49] Clarke GL, Bhattacherjee A, Tague SE, Hasan W, Smith PG. β-Adrenoceptor blockers increase cardiac sympathetic innervation by inhibiting autoreceptor suppression of axon growth. J Neurosci 2010;30:12446. doi:10.1523/JNEUROSCI.1667-10.2010.